

"TRAL-3" AND "TRAL-3M" IR LASER GAS ANALYZERS OF DIFFERENTIAL ABSORPTION

S.I. Dolgii, V.V. Zuev, S.V. Smirnov, and S.F. Shubin

*Institute of Atmospheric Optics,
Siberian Branch of the Academy of Sciences of the USSR, Tomsk
Received February 4, 1991*

The paper reports about modified versions of the "TRAL" laser gas analyzer of differential absorption. The specifications of these gas analyzers are given and their capabilities are described. An extended list of gases being probed and their minimum detectable concentrations detected by these devices is presented.

The intermediate IR spectral range of the electromagnetic radiation is well known to be of a considerable practical interest for laser gas analysis of the atmosphere, since bands or lines of absorption of virtually all atmospheric trace gases (ATG's) are presented in it.^{1,2} In addition, there are effective sources of discretely frequency-tunable coherent radiation in this range based on the CO and CO₂ lasers equipped with parametric frequency converters (PFC's).³⁻⁵

Previously we have reported⁴⁻⁷ about successful atmospheric measurements of the NH₃, O₃, C₂H₄, H₂O, CO, and NO concentrations in different climatic zones and under different ecological conditions by tunable CW

CO₂ lasers with the PFC's. These measurements were performed along the paths up to 3 km in length using a specular reflector and up to 0.125 km in length when operating with topographic targets (e.g., using edifice walls).

Recently, in our laboratory we have developed the models of the "TRAL-3" and "TRAL-3M" laser gas analyzers with differential absorption (LGADA) intended for remote and local high-sensitivity measurements of mass concentrations of the diverse ATG's of primary importance along both horizontal and slightly slanted paths. These models are now at their stage of operational development.

The block diagrams for both LGADA schemes are virtually the same (Fig. 1).

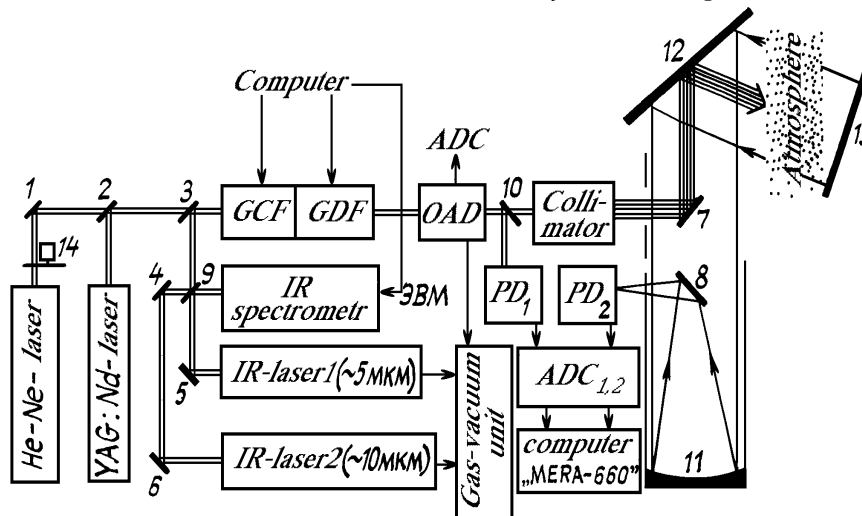


FIG. 1. Block diagram of the LGADA: movable mirrors (1-8), semi-transparent plates (9, 10), receiving mirror 30 cm in diameter (11), mirror-scanner (12), specular reflector (13) (in the case of "TRAL-3M" an option is possible with topographic target), and modulator (14).

However, different lasers (Fig. 2) are used as radiation sources in these models. For our first "TRAL-3" model we used low-pressure longitudinal-discharge CW tunable CO and CO₂ lasers with Q-switching and with generators of the summed and difference frequencies (GSF and GDF, respectively). As for the second "TRAL-3M" model, we made use of two pulsed tunable TEA CO₂ lasers with the GSF and GDF. In addition, one of the lasers was equipped with a generator of the second harmonic (GSH).

The available CW CO and CO₂ lasers have a narrow of stable lasing line with a half-width of about $2 \cdot 10^{-3} \text{ cm}^{-1}$. It is by 1-2 orders of magnitude narrower than the absorption line of the gas being probed in the intermediate IR range at atmospheric pressure. For this reason, the recorded values of spectral transmission of the atmospheric layer being probed are not distorted by the instrument function of the laser source.⁸ With 5-7 W average output power of the CO laser and 2-3 W of the CO₂ laser, a peak power of ~60 and

30 W, respectively, may be attained by Q-switching with a frequency of 10^2 – 10^3 Hz. In this case, the lasing pulse of 1–2 μ s width was realized. The efficiency of frequency transformation in the GSF of such lasers and GDF can then reach ~1%, so that the power of the pulse being probed will amount to ~0.6 W (neglecting the losses in the optical system). Because of such output power, measurements of the column gas concentration on the paths up to 2–3 km in length are possible only with the help of specular reflectors. However, such a probing power appears to be quite sufficient for using photodetectors with moderate sensitivity (e.g., pyroelectric detectors), if, naturally, the incident beam is completely intercepted.

The pulsed TEA CO₂ lasers, with their cavities at the working pressure of the mixture of ~300 Torr, have a half-line width of about $3 \cdot 10^{-2}$ cm⁻¹. This lasing line can be further narrowed by reducing the pressure of the mixture, but at the expense of a substantial decrease in power. The peak power of the 100 ns-pulse of the TEA CO₂ laser is 3–5 MW. The efficiency of frequency transformation in this laser exceeds 10% for the GSH and 1% for the GSF and GDF. In this case, the probing power approaches 300–500 kW for the GSH and about 30–50 kW for the GSF and GDF which is quite sufficient for measuring the ATG concentrations. The radiation is then recorded reflected from a remote topographic target using the high-sensitivity cooled photodetectors made of KPT, InSb, and InAs. It should be stressed that the recorded spectral transmission of the atmospheric layer being probed must be corrected since it is distorted because of finite width of the lasing laser line, which is additionally broadened by a factor of $\sim\sqrt{2}$ in each act of frequency transformation so that finally it becomes comparable in its width with the absorption lines of most gases.

Let us consider in more detail the optical part of the LGADA block diagram presented in Fig. 1. The PFC lasers emit in the following spectral intervals:

- 1) 9.2–10.8 μ m (the region of fundamental harmonics of the CO₂ laser),
- 2) 4.6–5.4 μ m (the region of second harmonics),
- 3) 3.1–3.6 μ m (the region of third harmonics), and
- 4) 8.0–13.1 μ m (the region of the difference frequencies between the harmonics from the second and first spectral intervals).

It should be emphasized that the CO₂ lasers used (both CW and pulsed lasers) are not sealed-off, so that the isotope composition of the gas mixture in laser tubes may be varied. Moreover, it is envisaged to introduce heated cells filled with CO₂ into the cavities of the pulsed TEA CO₂ lasers so that one may simultaneously switch over the secondary sequence band and the primary band near 4.3 μ m.

A scanning mirror directed the beam via a collimator onto either a topographic or specular reflector. Laser returns were then recorded by a pyroelectric detector or by a cooled photodetector depending on the type of the reflector used. The radiation wavelength is monitored by either an IR spectrometer or a panoramic spectrum analyzer (PSA). Availability of an optoacoustic detector (OAD) makes it possible to calibrate the LGADA and to measure the local gas concentrations in air parcels.

The He–Ne laser beam with a wavelength of 0.63 μ m is used to visualize the beam path and to adjust the optical system. Another wavelength of this laser (3.39 μ m) is used to measure the total concentration of hydrocarbons.

A pulsed YAG:Nd laser with a GSH wavelength of 0.53 μ m is used for range finding over the path being probed. In addition, its wavelengths 0.53 and 0.63 μ m are used to estimate the atmospheric mass aerosol content.

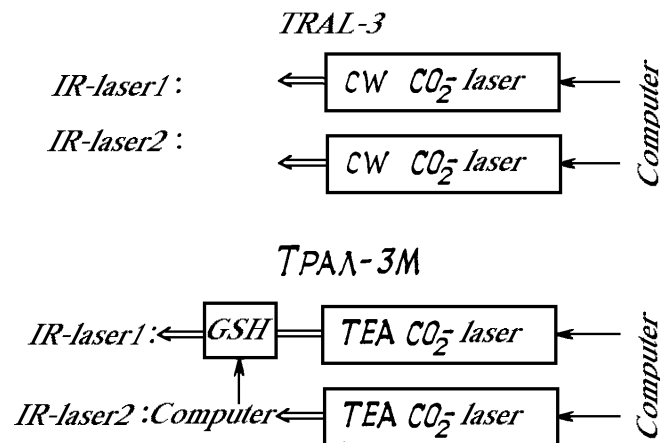


FIG. 2. Tunable IR molecular lasers for the "TRAL-3" and "TRAL-3M" models

TABLE I. Gases detected on the horizontal near-surface layer 1 km in length and their minimum detectable concentrations (MDC's) from the "TRAL-3" and "TRAL-3M" LGADA on-line and off-line absorption measurements.

Section	Gas	Lasing lines and their combinations		CDA,	MDC	MPC
		on-line	off-line	$\text{Cm}^{-1}\cdot\text{atm}^{-1}$	ppb	ppm
1	SF ₆	10P(16)	10P(10)	620.0	8(-2)	—
2	NH ₃	9R(30)	9R(28)	75.03	1	—
3	N ₂ H ₄	10P(32)	10P(34)	3.30	15	—
4	C ₆ H ₆	9P(30)	9P(26)	1.60	31	—
5	H ₂ O	10R(20)	10R(18)	0.001	165ppm	—
6	C ₂ H ₄	10P(14)	10P(12)	30.70	2	—
7	O ₃	9P(14)	9P(22)	11.10	5	—
1	8 C ₂ N ₅ SH	10R(26)	10P(20)	0.38	600	250
9	C ₂ H ₃ Cl	10P(22)	9R(18)	8.75	20	14
10	C ₂ HCl ₃	10P(20)	10R(20)	12.56	24	5
11	C ₂ Cl ₄	10P(34)	10R(24)	4.80	60	18
12	C ₂ H ₅ Cl	10R(16)	10P(20)	3.24	75	20
13	C ₂ H ₄ Cl ₂	10P(20)	10R(16)	0.51	550	120
14	C ₄ H ₅ Cl	10R(18)	9P(22)	9.05	45	12
15	CF ₂ Cl ₂	10P(32)	10P(12)	35.62	6	2
16	CFCl ₃	9R(22)	9P(18)	29.10	7	2
17	NO	2*10P(24)	2*10P(26)	1.98	41	—
18	CO	2*9P(24)	2*9P(26)	26.59	4	—
2	19 OCS	2*9P(30)	2*9P(14) ¹	113.9	1	—
20	CO ₂	10R(30)+9R(14)	2*9P(40)	0.023	4ppm	—
21	N ₂ O	9R(40)+9R(18) ²	2*9P(40)	18.07	6	—
3	22 HCl	2*10P(26)+10P(20)	2*10P(26)+10P(14)	34	3	3.350
23	NO ₂	2*10P(30)+9P(16)	2*10P(26)+9P(24)	4.00	25	1.064
24	CH ₄	2*9P(10)+10R(18)	2*9R(16)+10P(32)	43.70	2	—
25	H ₂ CO	2*10P(29)+10P(29) ³	2*10P(30)+10P(18)	23.10	4	0.408
4	26 SO ₂	2*9P(19) ³ -10P(14)	2*9P(22)-10P(16)	1.57	42	—
27	PH ₃	2*9P(28)-9R(34)	2*9P(34)-9R(12)	20.40	6	0.719
28	HNO ₃	2*10R(20)-9P(10)	2*10P(26)-10R(22)	9.42	11	1.252
29	C ₂ H ₂	2*10P(36)-9R(26)	2*10P(37) ³ -9R(36)	3.99	3	—
30	HCN	2*10P(38)-9R(38)	2*10P(37) ³ -9R(32)	4.50	22	0.272

¹ the C¹³O₂¹⁸ line.

² the C¹²O₂¹⁸ line.

³ the CO₂ sequence band.

The characteristics of both LGADA's are presented below. The general outlook of one of them ("TRAL-3M") is shown in Fig. 3. Tables I and II list the gases detected by the "TRAL-3" and the "TRAL-3M" LGADA's in probing on the horizontal atmospheric paths (emitter to reflector distance is up to 1 km), and their minimum detectable concentrations (MDC's). The minimum error in the recording of the optical signal is assumed to be 1%. The gases are grouped into sections corresponding to lasing spectra of these sources makes the "TRAL-3M" capable of probing SO₂ (Table I, Section 4, No. 26), while such a possibility is absent for the "TRAL-3". Conversely, one can probe HBr using the "TRAL-3" (Table I) but cannot do that with the "TRAL-3M". In addition, detection

sensitivities for both gases are different in the four spectral intervals of lasing of lasers with the PFC. The first two sections are common for both LGADA's except for items 20 and 21 (CO₂ and N₂O), which are absent from the "TRAL-3" list since for their realization two CO₂ lasers are needed. Sections three and four principally differ for the two systems though falling in a common spectral interval, the lasing spectra of the GSH of the CO laser and fundamental frequencies of the CO-laser are naturally different. A minor shift of the these two sections because the lasing lines fall into different spectral ranges having different coefficients of differential absorption (CDA's) on-line and off-line of these gases.



FIG. 3. The "TRAL-3M" LGADA: general outlook

TABLE II. Gases detectable in probing on the horizontal near-surface atmospheric layer 1 km in length by the "TRAL-3" LGADA (on-line and off-line absorption measurements) and their MDC's.

Section	Gas	Lasing lines and their combination		CDA, $\text{Cm}^{-1}\cdot\text{atm}^{-1}$	MDC, ppb	MPC, ppm
		on-line	off-line			
1	HCl	P(17)+10P(32)	P(15)+10P(16)	34.10	3	3.350
2	HBr	P(16)+10P(24)	P(15)+10P(30)	5.35	200	0.604
3	NO ₂	P(19)+9P(20)	P(21)+9P(26)	3.66	300	1.064
4	CH ₄	P(21)+9P(16)	P(19)+9P(24)	5.94	21	—
5	H ₂ CO	P(17)+10R(14)	P(18)+9P(18)	20.95	6	0.408
6	HNO ₃	P(16)—10R(20)	P(15)—10P(12)	9.42	110	1.252
4	7	PH ₃	P(16)—10P(28)	2.13	1 ppm	0.719
8	C ₂ H ₂	P(21)—9R(30)	P(18)—10R(18)	43.99	3	—
9	HCN	P(99)—9R(16)	P(14)—10R(22)	10.43	110	0.272

Note: Sections 1 and 2 are the same as in Table I, except for items 20 and 21. It appears disadvantageous to measure the CO₂ and N₂O concentrations at combined frequencies of the CO and CO₂ lasers, since the lasing lines do not exactly coincide with the absorption lines of these gases in that spectral range.

To search for informative lasing lines of the CO and CO₂ lasers and their combination frequencies in Sections 2, 3, and 4, numerical calculations were performed using the GEISA 9 atlas of spectral lines of atmospheric gases following the technique described in Refs. 10 and 11. The data for Section 1 are borrowed from the well-known publications.^{1,2,12}

In conclusion it should be noted that the list of gases being probed is far from being complete since the reliable data on the absorption lines and bands of many other gases are unavailable. To be sure, the "TRAL-3M" has an

advantage over the "TRAL-3" in both the number of gases it probes and in the capability of a wider choice of paths being probed. It is even capable of quasispatial resolution if remote topographic targets located at a different distances are employed. However, the "TRAL-3" with its CW lasers and uncooled photodetectors has better noise proof, and is more reliable and cheap.

The design of both LGADA's, their mass and overall dimensions as well as the energy consumption parameters are specifically intended for mounting in a van of a truck (see Table III).

Specifications**Transmitter**

"TRAL-3" "TRAL-3M"

Maximum power of
probing pulse at:

3.1–3.6 μm (GSF)	< 0.6 W	50 kW
4.6–5.4 μm (GSH)	< 0.6 W	500 kW
8.0–13.1 μm (GDF)	< 0.6 W	50 kW
9.2–10.8 μm	30–60 W	5 MW
Pulsewidth	1–2 μs	100 ns
Pulse repetition frequency	100–150 Hz	1–5 Hz

Detector

Telescope diameter	0.3 m
Telescope focal length	1 m
Field-of-view angle of the telescope	~5 mrad
Limiting sensitivity:	
cooled photodetector	$10^{-9} \text{ cm Hz}^{1/2} \cdot \text{W}^{-1}$
pyroelectric detector	$10^{-5} \text{ V} \cdot \text{W}^{-1}$
optoacoustic detector	$10^{-9} \text{ cm}^{-1} \cdot \text{W}$
Concentration sensitivity	from several ppb to tens of ppm depending on a gas

Recording and data processing system

Analog-to-digital converter:	
number of channels	4
sampling frequency	20 MHz
Data processing	minicomputer

Range of action and direction of probing

Path length	~2 km	~4 km
Elevation angle	from -10°	to $+60^\circ$
Azimuth		360°
Voltage	380/220 V (50 Hz)	
Consumed power	~3.5 kW	

Overall dimensions

Optomechanical unit	2.5×0.6×2.0 m
Power supply unit	1.0×1.0×1.5 m
Recording, data processing, and control unit	1.0×1.0×1.5 m
Gas-vacuum unit	0.5×1.0×1.0 m
Net mass	~650 kg

The authors express their sincere gratitude to O.V. Kharchenko for his assistance in numerical computations.

REFERENCES

1. R.A. McClatchey, W.S. Benedict, S.A. Clough, et al., Tech. Rep. AFCRL-TR-73-0096, ERP 434, 1973.
2. L.S. Rothman, R.R. Gamache, A. Goldman, et al., Appl. Opt. No. 26, 4058 (1987).
3. Yu.M. Andreev, P.P. Geiko, V.V. Zuev, et al., Opt. Atm. 1, No. 2, 51–56 (1988).
4. S.I. Dolgii, L.P. Kudinova, A.A. Mitsel', et al., in: *Systems for Automation of the Experiment in Atmospheric Optics*, Institute of Atmospheric Optics, Siberian Branch of the Academy of Sciences of the USSR, Tomsk, 1980, pp. 67–68.
5. Yu.M. Andreev, P.P. Geiko, A.I. Gribenyukov, et al., Opt. Atm. 1, No. 3, 20–26 (1988).
6. I.V. Samokhvalov, Yu.D. Kopytin, I.I. Ippolitov, et al., eds., *Laser Sounding of the Troposphere and Underlying Surface* (Nauka, Novosibirsk, 1987), pp. 107–122.
7. Yu.M. Andreev, I.L. Vasin, P.P. Geiko, et al., in: "Vertikal'-86" and "Vertikal'-87" *Complex Experiments*, Tomsk Scientific Center, Siberian Branch of the Academy of Sciences of the USSR, Tomsk, 1989, pp. 77–94.
8. V.V. Zuev and O.A. Romanovskii, "On account of systematic errors in lidar method of differential absorption," VINITI, No. 4675–B87, June 25, (1987).
9. N. Husson, A. Chedin, N.A. Scott, et al., Ann. Geophys., Fass. 2, Ser. A.
10. Yu.M. Andreev, V.V. Zuev, and O.A. Romanovskii, "Automated search system for laser-gas-analyzer optimal wavelengths using differential absorption," VINITI, No. 4059–B88, March 19, (1988), Parts I and II.
11. V.V. Zuev and O.A. Romanovskii, Opt. Atm. 1, No. 12, 29–32 (1988).
12. A. Mayer, T. Comera, H. Charpentier, and C. Taussand, Appl. Opt. 17, No. 3, 391–393 (1978).